Novel UF-OFDM transmitter: significant complexity reduction without signal approximation

Jérémy Nadal, Charbel Abdel Nour, Amer Baghdadi

Novel UF-OFDM transmitter: significant complexity reduction without signal approximation

Jeremy Nadal *Student Member, IEEE*, Charbel Abdel Nour *Member, IEEE*, Amer Baghdadi *Senior Member, IEEE*

***Abstract*—The upcomping 5th generation (5G) of mobile communication system aims to support multiple new services and use cases towards a flexible and unified connectivity. In order to meet the corresponding requirements, Universal-Filtered Orthogonal Frequency-Division Multiplexing (UF-OFDM) was proposed to replace the existing waveform since it combines the advantages related to OFDM with better spectral properties and with improved robustness against time-frequency misalignments. However, its main drawback resides in the computational complexity of the transmitter reaching up to 200 times that of OFDM if no simplification is applied. While still of high complexity, most efficient simplification techniques significantly compromise the achieved spectral confinement through signal approximations. In this context, a novel low-complexity UF-OFDM transmitter without any signal quality loss is proposed. For small subband sizes, the complexity becomes comparable to OFDM regardless of the number of allocated subbands. Furthermore, the proposed transmitter architecture is flexible and can be easily adapted to support OFDM modulation.**

***Index Terms*—OFDM, UF-OFDM, multicarrier modulation, 5G**

I. Introduction

The 5th generation (5G) of mobile communication systems is foreseen to support multiple new services while coexisting with the typical mobile broadband service of 4G/Long Term Evolution (LTE). For internet-of-things applications, massive Machine-Type Communication (mMTC) service is introduced, adding specific requirements such as the support of imperfect synchronization. Other applications, like Mission Critical Communication (MCC), may require the support of low-latency communication, which can be achieved by reducing the time transmission interval. Therefore, multiple waveform parameters on the same carrier (often referred to as numerology) may be required to support all types of applications, which raises the issue of their coexistence. To partly answer these new challenges, novel waveforms have been designed and proposed for the upcoming 5G standard.

Universal-Filtered Orthogonal Frequency-Division Multiplexing (UF-OFDM) is one of the key 5G candidate waveforms and was originally proposed in [1]. The original idea of this waveform consists in grouping multiple allocated subcarriers into subbands, independently filtered in the time domain. Thus, the filtering is realized subband-wise and not subcarrier-wise as in the Filter-Bank Multi-Carrier with Offset-Quadrature Amplitude Modulation (FBMC/OQAM) [2]. UF-OFDM shows advantages for low-latency communications (MCC services) and enables the use of open-loop synchronization to save bandwidth and energy [3]. In addition, unlike other 5G candidate waveforms such as FBMC/OQAM, the majority of the techniques employed in OFDM can be reused without significant modifications. For instance, the techniques presented in [4] are applicable to UF-OFDM.

However, the main drawback of the UF-OFDM modulation resides in the complexity of the transmitter. The baseline implementation is estimated to be up to 200 times more computationally complex than OFDM [5]. Some recent techniques have been proposed to reduce the computational complexity [5][6]. However, these still require up to 10 times the complexity of OFDM [5], while calling for an approximated signal implying a penalty in bit error rate and in spectral confinement.

In this work, we propose a novel and significantly simplified UF-OFDM transmitter able to generate a signal exempt from any approximation when compared to the baseline solution. The complexity reduction is obtained by exploiting two main ideas:

- First, the processing related to the subbands and the processing related to the subcarriers are separated. The subband processing can be performed at a low complexity by computing multiple Inverse Fast Fourier Transforms (IFFTs) of a small size.
- Second, the subcarrier processing is subdivided into 3 parts corresponding to the generation of the prefix, the core and the suffix parts of the UF-OFDM symbol. The core part of the signal can be efficiently generated using multiple IFFTs of small size, and the suffix part can be simply deduced from the prefix and core parts of the signal, which further lowers the complexity.

The originality of the proposed technique resides in avoiding redundant operations performed by the baseline technique without altering the original signal. Thus, being mathematically identical to the baseline solution, the proposed technique does not have any impact on the Out-Of-Band Power Leakage (OOBPL) with respect to the baseline solution. To the best of our knowledge, this is the first time that such UF-OFDM technique is proposed in the literature. Furthermore, the technique can be easily adapted to perform OFDM modulation and thus enables direct compatibility with 4G/LTE.

The rest of the paper is organized as follows. Section II gives a technical description of the UF-OFDM baseline transmitter and the solutions provided in the literature to reduce the computational complexity. Section III details the proposed UF-

J. Nadal, C. Abdel Nour and A. Baghdadi are with IMT Atlantique, CNRS Lab-STICC, UBL, F-29238 Brest, France (e-mail:{firstname.lastname}@imt-atlantique.fr)

Part of this work has been performed in the framework of the Horizon 2020 project FANTASTIC-5G (ICT-671660), which is partly funded by the European Union.

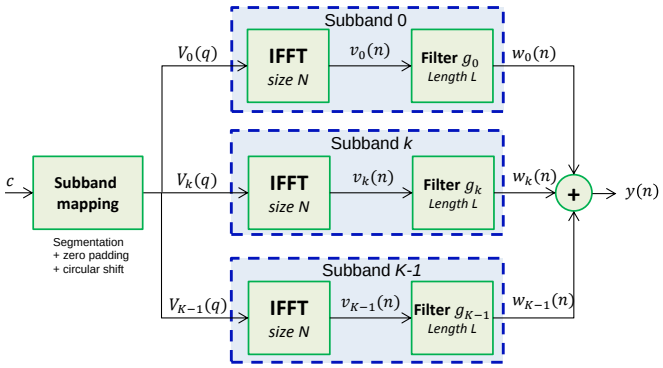

Fig. 1. Baseline UF-OFDM transmitter

OFDM technique. Section IV provides computational complexity analysis and comparisons with the existing techniques in the literature. Finally, Section V concludes the paper.

II. UF-OFDM TECHNICAL DESCRIPTION AND EXISTING SOLUTIONS

A. Baseline UF-OFDM transmitter

The principle of the UF-OFDM modulation is to group the complex samples carrying information into several subbands, each composed of Q subcarriers. These complex samples can be, for instance, symbols from a Quadrature Amplitude Modulation (QAM) constellation. A maximum of $K = \lfloor N/Q \rfloor$ subbands carrying Q subcarriers can be used, where N is the total number of subcarriers, and $\lfloor x \rfloor$ represents the largest integer less than or equal to x (floor operator). The secondary sidelobes (residual power outside the subbands) of each subband are attenuated by independent subband-wise filtering of length L samples. The resulting discrete time signal represents the sum of the signals emanating from the filtered subbands. It forms the UF-OFDM symbol, composed of $N+L-1$ samples. The baseline UF-OFDM transmitter is represented in Fig. 1.

Let c be a vector of length BQ containing the complex symbols to be transmitted. To map each symbol in c to the allocated subbands, we first group the symbols into B subsets $c_i(q)$, for $q \in [\![0, Q-1]\!] (= \{0, 1, ..., Q-1\})$, such that $c_i(q) = c(q+Qk)$. In order to support an arbitrary assignment of symbol groups to subbands, we define a bijective function $i = \phi(k)$ that maps the index $k \in \Omega_B$ of an allocated subband to a symbol group i, where Ω_B is the set of the B allocated subband indexes. The segmented samples $s_k(q)$ for subcarrier index q of subband $k \in [\![0, K-1]\!]$ can then be expressed as

$$s_k(q) = \begin{cases} c_{\phi(k)}(q) & , k \in \Omega_B, \\ 0 & , k \notin \Omega_B. \end{cases} \quad (1)$$

In the frequency domain, a total of N subcarriers are defined. Thus, the samples $s_k(q)$ must be zero padded with $N-Q$ zeros:

$$s'_k(q) = \begin{cases} s_k(q), & q \in [\![0, Q-1]\!] \\ 0, & q \in [\![Q, N-1]\!], \end{cases},$$

where $s'_k(q)$ represents the zero padded version of s_k. Then, a circular shift of $kQ + k_0$ samples is applied, to move each subband into its respective subband position in the frequency domain. The obtained signal $V_k(q)$ is expressed as

$$V_k(q) = s'_k(\mathrm{mod}_N(q - (kQ + k_0))),$$

where mod_N corresponds to the modulo N operator, $k_0 \in [\![0, Q-1]\!]$ corresponds to the value of the shift in number of subcarriers. This shift at subcarrier level can be used to move each subband to the center of the allocated bandwidth. For each index k, the $V_k(q)$ signal for subband k contains N samples, one for each subcarrier. However, only Q subcarriers, defining the subband number k, carry the information to transmit. The remaining subcarriers are not used (zero padded). Thus, each subband is isolated from the others, and can be processed independently. The subband mapping block represented in Fig. 1 corresponds to the segmentation, the zero padding and the circular shift operations detailed above.

Next, the $V_k(q)$ samples are transformed to the time domain using an IFFT of size N for each subband k:

$$v_k(n) = R_N(n) \sum_{q=0}^{N-1} V_k(q) e^{j2\pi \frac{qn}{N}}, n \in [\![0, N+L-2]\!], \quad (2)$$

where L is the length of the impulse response of the subband filter and $R_N(n)$ represents the rectangular window of length N: $R_N(n) = 1, n \in [\![0, N-1]\!]$ else 0. The windowing operation has negligible complexity and is omitted from Fig. 1 for clarity.

Then, as shown in Fig. 1, each subband is filtered separately using a linear convolution by the impulse response of the subband filter g_k:

$$w_k(n) = \sum_{l=0}^{L-1} g_k(l) v_k(n-l), n \in [\![0, N+L-2]\!],$$

where $w_k(n)$ represents the result of the filtering operation. The impulse response of these filters can be obtained from the impulse response of a common filter $f_Q(n)$, that we refer to as the subband prototype filter, as

$$g_k(n) = f_Q(n) e^{j2\pi \frac{kQn}{N}}, n \in [\![0, L-1]\!].$$

In fact, the impulse response of the subband filter number k corresponds to the impulse response of the subband prototype filter, shifted in frequency by kQ subcarriers. This frequency shift aligns the frequency response of the filter to the subband position k. Furthermore, the frequency response of the subband prototype filter f_Q is centered around the subcarrier index $Q/2$ if Q is even (or around $(Q-1)/2$ if Q is odd), corresponding to the center of a subband. If $f(n)$ is the impulse response of the subband prototype filter, then, for $n \in [\![0, L-1]\!]$, we have

$$f_Q(n) = \begin{cases} \frac{Q}{2} & Q \text{ even}, \\ \frac{Q-1}{2} & Q \text{ odd}. \end{cases} \quad (3)$$

In the literature, a typical choice for the subband prototype filter is the Dolph-Chebyshev filter [7]. More recently, a specific filter design has been studied to reduce the out-of-band power spectral leakage for UF-OFDM [8] and to improve robustness against frequency/timing-offset errors [9].

Finally, the $N+L-1$ time domain samples of the filtered subbands are summed together to form the UF-OFDM symbol $y(n)$, implicitly sampled at the frequency f_s:

$$y(n) = \sum_{k=0}^{K-1} w_k(n), n \in [\![0, N+L-2]\!]. \quad (4)$$

In a practical implementation, only the B allocated subbands are considered to calculate the UF-OFDM symbol, since the $B-K$ other subbands correspond to zero-valued samples in the time domain:

$$y(n) = \sum_{k \in \Omega_B} w_k(n), n \in [\![0, N+L-2]\!].$$

While this solution has an acceptable computational complexity for a limited number of allocated subbands, it becomes computationally expensive when the number of allocated subbands increases. Indeed, the computation of one subband requires the use of an IFFT of size N (complexity in $\mathcal{O}(N \log_2 N)$) and a linear convolution operation (complexity in $\mathcal{O}(L^2 + LN)$)). Therefore, the computation of only one subband already requires a larger number of operations than needed to compute one OFDM symbol (one IFFT of size N), due to the complexity overhead introduced by the linear convolution of the subband filtering stage. These operations have to be repeated for each allocated subband. For $B = 100$, which corresponds to the maximum number of resource blocks ($Q = 12$) that can be allocated in 4G/LTE, the computational complexity exceeds 200 times the computational complexity of the OFDM transmitter [5].

Few techniques with lower computational complexity have been investigated in the literature. Among existing techniques, one applies the subband filtering in the frequency domain instead of the time domain, and a second approximates the UF-OFDM signal by decomposing it into multiple windowed OFDM signals that are then summed. These approaches are reviewed in the following subsections. They reduce the computational complexity of the UF-OFDM transmitter, but at the cost of a degradation of the original signal.

B. Frequency domain UF-OFDM transmitter

In this approach [5], the filtering stage and the summation of all subbands are computed in the oversampled frequency domain (FD), i.e. before the IFFT. We refer to this technique as FD UF-OFDM in this paper. The IFFT size is multiplied by N_{OS} which corresponds to a chosen oversampling factor. In general, this parameter is set to $N_{OS} = 2$ since this value provides the best compromise between approximation errors and computational complexity [5]. Additionally, the computation of the filtering stage in the frequency domain requires an IFFT of size N_0 and an FFT of size $N_{OS}N_0$ for each subband, where $N_0 \geq Q$ is a design parameter. Note that the computational complexity increases with the value of N_0. However, the impact on the OOBPL is reduced with respect to the baseline solution. Finally, only $N+L-1$ samples, corresponding to the length of one UF-OFDM symbol, are kept after the computation of the IFFT of size $N_{OS}N$.

Since this technique uses a smaller IFFT size per processed subband than the baseline solution presented in Subsection II-A, the computational complexity is significantly reduced. However, it is still higher than that of OFDM, due to the use of an IFFT of size $N_{OS}N$ instead of N, and due to the additionnal small IFFT/FFT of size N_0 and $N_{OS}N_0$ for each allocated subband. According to [5], the required number of multipliers and adders can be up to 10 times higher than in the case of OFDM.

C. Time domain windowed UF-OFDM transmitter

The second simplified UF-OFDM transmitter is based on a time-domain processing without oversampling [6]. We refer to it as Time-Domain-Windowed (TDW) UF-OFDM in this paper. It consists of subdividing each subband into small groups of subcarriers, each group being subcarrier-wise filtered by a dedicated filter. This subcarrier-wise filtering can be efficiently implemented by using a windowing operation in the time domain (after IFFT). The impulse response of the common group filter is used as window coefficients. It results into an approximated UF-OFDM signal. This results in an approximation of the UF-OFDM signal, which is obtained by summing multiple windowed OFDM symbols as

$$y(n) \approx \sum_{i=0}^{N_w-1} w_i(n) u_i(n), n \in [\![0, N+L-2]\!].$$

The computational complexity increases linearly with the number of windows being employed (in $\mathcal{O}(N_W N \log_2 N)$) comparable to N_W times the complexity of a typical OFDM transmitter. However, increasing the number of windows decreases the approximation errors and reduces the OOBPL. Similarly to the FD UF-OFDM technique, a trade-off between approximation errors and computational complexity must be considered.

III. Proposed low-complexity UF-OFDM transmitter

For all simplified UF-OFDM transmitters, a compromise must be found between performance and complexity. Thus, a novel UF-OFDM technique that reduces the computational complexity to an acceptable level without altering the original signal is of high interest. The proposed approach achieves this goal by exploiting a specific decomposition into subband and subcarrier processing.

A. Description of the proposed technique

The proposed technique exploits two main ideas to reduce the computational complexity of the UF-OFDM baseline implementation. First, the required UF-OFDM processing is divided into subband-wise and subcarrier-wise computations in such a way to avoid redundant operations, especially when

a high number of subbands is allocated. The second core idea is to divide the UF-OFDM symbol into prefix, core and suffix parts, which are efficiently processed by exploiting the previous decomposition into subband-wise and subcarrier-wise processing. The suffix part is deduced from the core part and the prefix part by a simple subtraction. These two core ideas exploit the UF-OFDM baseline equation. Therefore the resulting signal is not altered when compared to this baseline solution.

By using the circular shift property of the IFFT, (2) can be rewritten as

$$\begin{aligned} v_k(n) &= R_N(n) e^{j2\pi \frac{(kQ+k_0)n}{N}} \sum_{q=0}^{N-1} s'_k(q) e^{j2\pi \frac{qn}{N}} \\ &= e^{j2\pi \frac{k_0 n}{N}} R_N(n) \sum_{q=0}^{Q-1} s_k(q) e^{j2\pi \frac{(q+kQ)n}{N}}. \end{aligned} \quad (5)$$

To simplify the development of the following equations, the number of shifted subcarriers is assumed to be equal to zero ($k_0 = 0$). This constraint does not alter the following demonstration, since the frequency shifted UF-OFDM symbol can be recovered by applying a simple linear phase rotation to the unshifted UF-OFDM symbol. Thus, expression (4) of the UF-OFDM symbol combined with (5) becomes, for $n \in [\![0, N+L-1]\!]$,

$$\begin{aligned} y(n) = \sum_{k=0}^{K-1} \sum_{l=0}^{L-1} \Big(& f_Q(l) e^{j2\pi \frac{kQl}{N}} R_N(n-l) \\ & \times \sum_{q=0}^{Q-1} s_k(q) e^{j2\pi \frac{q+kQ}{N}(n-l)} \Big). \end{aligned}$$

It is possible to simplify this equation by rearranging the order of the three summations as

$$\begin{aligned} y(n) &= \sum_{q=0}^{Q-1} \sum_{l=0}^{L-1} \Big(f_Q(l) R_N(n-l) \\ &\quad \times \sum_{k=0}^{K-1} s_k(q) e^{j2\pi \frac{q(n-l)+kQ(n-l)+kQl}{N}} \Big) \\ &= \sum_{q=0}^{Q-1} \Big(f_q(n) \sum_{k=0}^{K-1} s_k(q) e^{j2\pi \frac{kQn}{N}} \Big), \end{aligned} \quad (6)$$

with

$$f_q(n) = \sum_{l=0}^{L-1} f_Q(l) R_N(n-l) e^{j2\pi \frac{q(n-l)}{N}}. \quad (7)$$

These equations are further developed, by assuming that the total number of subcarriers across all the subbands (N) can be decomposed into an integer number of subbands ($\text{mod}_Q(N) = 0$). Then we have $K = N/Q$, and (6) can be rewritten as

$$y(n) = \sum_{q=0}^{Q-1} f_q(n) x_q(n), \quad (8)$$

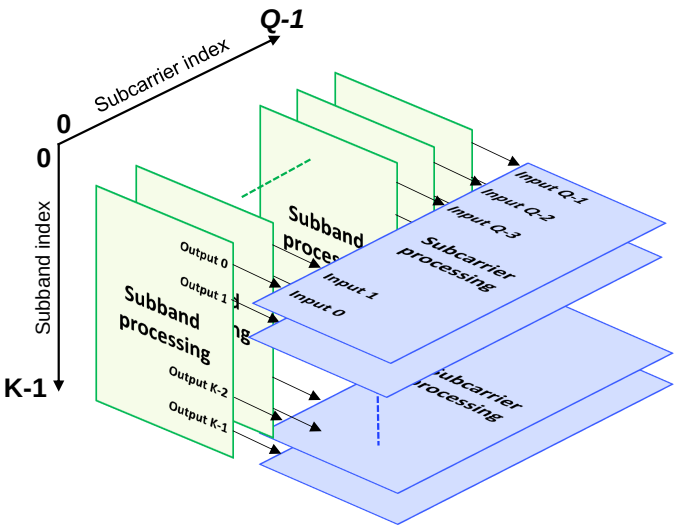

Fig. 2. Separation of the subband processing and the subcarrier processing

with

$$x_q(n) = \sum_{k=0}^{K-1} s_k(q) e^{j2\pi \frac{kn}{K}}, \quad (9)$$

where $x_q(n)$ corresponds to the IFFT of size K of the samples related to the subcarrier number q of each of the K subbands. Then, by exploiting the fact that the IFFT of size K is a periodic function of K samples, the first N samples of the UF-OFDM symbol ($y(n)$) can be decomposed into Q fragments of K samples ($N = K \times Q$). The fragmented symbol $y_p(n') = y(n' + pK)$, for $n' \in [\![0, K-1]\!]$ and $p \in [\![0, Q-1]\!]$, its expression can be written as

$$y_p(n') = \sum_{q=0}^{Q-1} f_q(n' + pK) x_q(n'). \quad (10)$$

Thus, it is possible to separate the processing of each subband (for a given subcarrier index) and the processing of each subcarrier (for a given subband index), as illustrated in Fig. 2. The subband processing consists of calculating the $x_q(n')$ samples from (9) using an IFFT of size K. This processing must be repeated for all the Q subcarrier indexes, and K samples are generated per subband processing to obtain a total of N samples. Then, the UF-OFDM symbol is generated by the subcarrier processing that computes the $y_p(n')$ samples (for each subcarrier index q) from the subband processing according to (10).

This separation between subband processing and subcarrier processing is the first core idea of the proposed technique and enables to reduce the computational complexity to process the first N samples of the UF-OFDM symbol. Indeed, the required number of operations scales in $\mathcal{O}(N\log_2(K))$ which is less computationally demanding than the processing of one IFFT of size N (in $\mathcal{O}(N\log_2(N))$). Furthermore, the computational complexity does not depend anymore on the number of allocated subbands B. However, the corresponding

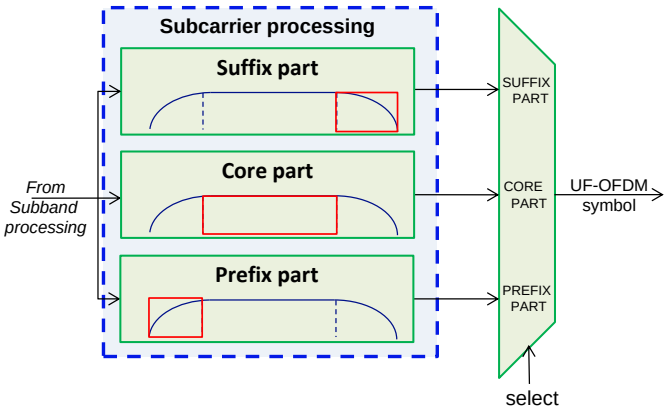

Fig. 3. Decomposition of the subcarrier processing into a prefix, core, and suffix parts.

overhead introduced by the subcarrier processing (complexity in $\mathcal{O}(Q(N+L))$) is not negligible.

In fact, it is possible to further simplify the subcarrier processing by decomposing the UF-OFDM symbol into 3 distinct parts, as shown in Fig. 3:

- The first part of the UF-OFDM symbol corresponds to the first L samples processed by the linear convolution operation (subband filtering). This part of the UF-OFDM symbol has a signal envelope that corresponds to the shape of the first half of the impulse response of the subband prototype filter. We refer to this part as the prefix part of the UF-OFDM symbol.
- The second part of the UF-OFDM symbol, which we call the core part, is composed of $N-L$ samples and corresponds to the samples in the interval $n \in [\![L, N-1]\!]$. This part of the symbol can be seen as the result of a circular convolution applied to the output of the IFFTs of size N of the UF-OFDM baseline solution.
- Finally, the last part of the UF-OFDM symbol corresponds to the last $L-1$ samples processed by the linear convolution operation. This part of the UF-OFDM symbol has a signal envelope that corresponds to the shape of the second half of the impulse response of the subband prototype filter. We refer to this part as the suffix part of the UF-OFDM symbol.

The core part of the UF-OFDM symbol can be efficiently computed by noting that (7) can be simplified when $n \in [\![L, N-1]\!]$ as

$$f_q(n) = e^{j2\pi\frac{qn}{N}} \sum_{l=0}^{L-1} f_Q(l) e^{-j2\pi\frac{ql}{N}}.$$

Furthermore, these coefficients can be segmented as

$$f_q(n'+pK) = e^{j2\pi\frac{qp}{Q}} F_q(n'),\ (n'+pK) \in [\![L, N-1]\!], \quad (11)$$

with

$$F_q(n') = e^{j2\pi\frac{qn'}{N}} \sum_{l=0}^{L-1} f_Q(l) e^{-j2\pi\frac{ql}{N}}. \quad (12)$$

The coefficients $F_q(n')$ can be obtained by applying an FFT of size N on the impulse response of the subband prototype filter $f_Q(l)$. From the result of this FFT, only the first Q coefficients are useful (since $q \in [\![0, Q-1]\!]$). Then, a linear phase rotation is applied (the exponential term) for each subcarrier index q. In total, $Q \times K = N$ coefficients are generated. These coefficients constitute the filter core coefficients.

By combining the equation of the segmented samples (10) with the equation of the segmented filter coefficients (11), we obtain

$$y_p(n') = \sum_{q=0}^{Q-1} z_q(n') e^{j2\pi\frac{qp}{Q}},\ (n'+pK) \in [\![L, N-1]\!], \quad (13)$$

with

$$z_q(n') = F_q(n') x_q(n'). \quad (14)$$

The $z_q(n')$ samples are obtained after multiplication of the $x_q(n')$ samples by the filter core coefficients $F_q(n')$ defined in (12), and can be seen as a windowing operation. Then, the n'-th samples of each of the Q fragments are calculated using an IFFT of size Q of the windowed samples $z_q(n')$ across the Q subcarriers. With the proposed separation between subband and subcarrier processing, it is then possible to efficiently compute the core part of the UF-OFDM symbol by using K IFFTs of size Q, reducing the computational complexity to $\mathcal{O}(N\log_2(Q))$. As shown in Fig. 2, the Q input samples of the subcarrier processing number $n' \in [\![0, K-1]\!]$ corresponds to the output samples number n' of the Q subbands processing. Thus, for the subcarrier processing, the order in which the subcarrier and subband samples are processed is interleaved when compared to the subband processing. Each subcarrier processing requires one windowing stage and one IFFT of size Q to generate Q samples of the segmented core part. Then, the core part is recovered using the following equation:

$$y_{\text{core}}(n) = y_{\lfloor n/K \rfloor}(\text{mod}_K(n)). \quad (15)$$

After the computation of the core part ($n \in [\![L, N-1]\!]$), the prefix ($n \in [\![0, L-1]\!]$) and suffix ($n \in [\![N, N+L-2]\!]$) parts of the UF-OFDM symbol must be calculated. When $n_p \in [\![0, L-1]\!]$, n_p being the sample index of the prefix part, (7) becomes

$$\begin{aligned} f_q(n_p) &= e^{j2\pi\frac{qn_p}{N}} \sum_{l=0}^{n_p} f_Q(l) e^{-j2\pi\frac{ql}{N}} \\ &= P_q(n_p). \end{aligned} \quad (16)$$

The $P_q(n_p)$ coefficients constitute the prefix tail coefficients. An efficient way to calculate these coefficients is by exploiting the following:

$$\begin{aligned} P_q(n_p+1) &= e^{j2\pi\frac{q(n_p+1)}{N}} \sum_{l=0}^{n_p+1} f_Q(l) e^{-j2\pi\frac{ql}{N}} \\ &= f_Q(n_p+1) + P_q(n_p) e^{j2\pi\frac{qn_p}{N}}. \end{aligned}$$

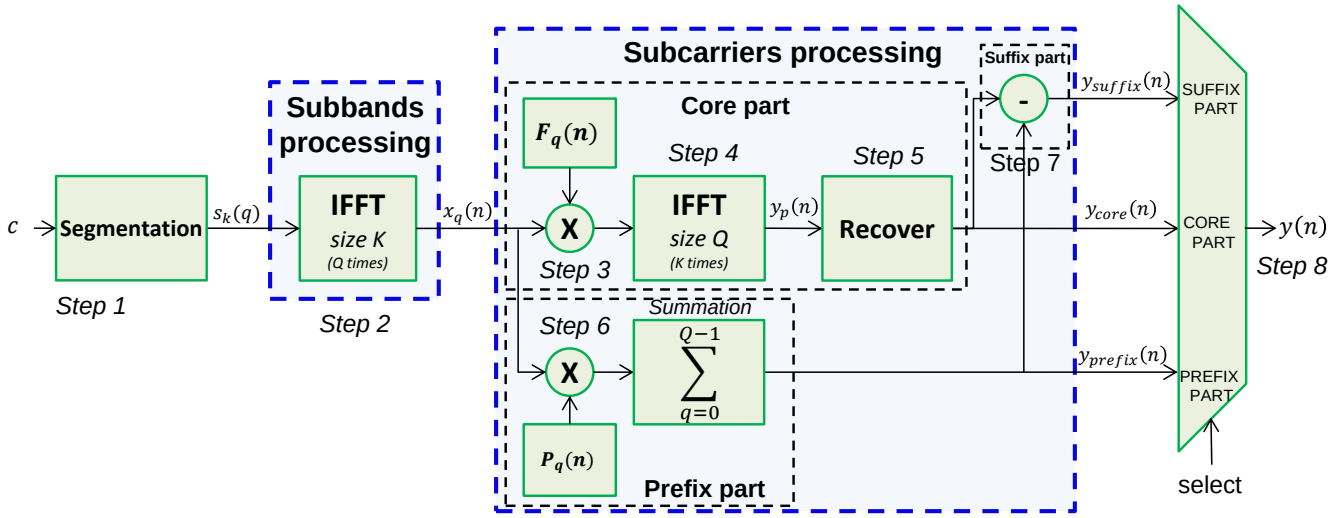

Fig. 4. Proposed low-complexity UF-OFDM transmitter

Thus, the prefix tail coefficient number $n_p + 1$ can be recursively calculated by adding the sample number $n_p + 1$ of the impulse response of the subband prototype filter to the previously calculated prefix tail coefficients (number n_p), after multiplication by a linear phase rotation term. This efficient way to compute the prefix tail coefficients is interesting if there is a requirement to generate these filters in real time, for instance to support multiple types of filter coefficients and/or filter lengths. Otherwise, such coefficients can be simply pre-computed and stored in a Look-Up-Table (LUT).

Then, the prefix part of the UF-OFDM symbol $y_{\text{prefix}}(n_p)$ can be deduced from equation (8)

$$y_{\text{prefix}}(n_p) = \sum_{q=0}^{Q-1} P_q(n_p) x_q(n_p), n_p \in [\![0, L-1]\!]. \quad (17)$$

The samples corresponding to the prefix part of the UF-OFDM symbol are obtained by:

- Multiplying the $x_q(n_p)$ samples by the prefix tail coefficients $P_q(n_p)$, which can be seen as a windowing operation.
- Summing over the subcarrier index q all the Q windowed samples for each sample n of the prefix part.

The generation of the prefix part can be included in the subcarrier processing of Fig. 2 since the interconnections between the subband and the subcarrier processing are unchanged. The sample number n of the prefix part is generated from the output number n of each of the Q subband processing blocks.

For the suffix part of the UF-OFDM symbol, we have $n_s \in [\![N, N+L-2]\!]$, and in that case (7) becomes

$$\begin{aligned} f_q(n_s) &= e^{j2\pi \frac{qn}{N}} \sum_{l=n_s-N+1}^{L-1} f_Q(l) e^{-j2\pi \frac{ql}{N}}, \\ &= S_q(n_s). \end{aligned}$$

The coefficients $S_q(n_s)$ denote the suffix tail coefficients. These coefficients can be deduced by subtracting the filter core coefficients from the prefix tail coefficients as

$$\begin{aligned} S_q(n_s) &= e^{j2\pi \frac{qn}{N}} \Big(\sum_{l=0}^{L-1} f_Q(l) e^{-j2\pi \frac{ql}{N}} - \sum_{l=0}^{n_s-N} f_Q(l) e^{-j2\pi \frac{ql}{N}} \Big), \\ &= F_q(n_s) - P_q(n_s - N). \end{aligned}$$

Then, the suffix part of the UF-OFDM symbol can be deduced from (8)

$$y(n_s) = \sum_{q=0}^{Q-1} \Big(F_q(n_s) - P_q(n_s - N) \Big) x_q(n_s), \; n_s \in [\![N, N+L-2]\!].$$

Due to the periodicity of $x_q(n_s)$ and $F_q(n_s)$, the above equation is equivalent to

$$y(n_s) = \sum_{q=0}^{Q-1} \Big(F_q(n_s - N) - P_q(n_s - N) \Big) x_q(n_s - N).$$

Thus, the suffix part $y_{\text{suffix}}(n_s)$ can be expressed as follows for $n_s \in [\![0, L-2]\!]$:

$$\begin{aligned} y_{\text{suffix}}(n_s) &= y(n_s + N) \\ &= \sum_{q=0}^{Q-1} \Big(F_q(n_s) - P_q(n_s) \Big) x_q(n_s) \\ &= y_{\text{core}}(n_s) - y_{\text{prefix}}(n_s), \end{aligned} \quad (18)$$

where the support of $y_{\text{core}}(n)$ is extended to $n \in [\![0, N-1]\!]$ instead of $[\![L, N-1]\!]$ as in (13). The samples in the interval $n \in [\![0, L-1]\!]$ are only generated to compute the suffix part of the UF-OFDM symbol. This shows that the suffix part of the UF-OFDM symbol can be simply deduced by subtracting the core part of the UF-OFDM symbol from its prefix part, avoiding additional computational complexity overhead.

Finally, the complete UF-OFDM symbol is obtained by the concatenation of the prefix part, the core part and the suffix part:

$$y(n) = \begin{cases} y_{\text{prefix}}(n), & n \in [\![0, L-1]\!] \\ y_{\text{core}}(n), & n \in [\![L, N-1]\!] \\ y_{\text{suffix}}(n-N), & n \in [\![N, N+L-2]\!] \end{cases} \quad (19)$$

The proposed UF-OFDM transmitter is illustrated in detail in Fig. 4 and can be summarized by the 8 steps:

Step 1) Segment the complex source symbols c into B subbands of Q subcarriers.

Step 2) Compute the IFFT of size K of the segmented samples (from step 1) corresponding to the qth subcarrier of each of the K subbands. This IFFT has to be computed Q times, for each subcarrier $q \in [\![0, Q-1]\!]$ to obtain the $x_q(n)$ samples.

Step 3) Multiply the $x_q(n')$ samples (from step 2) by the subband prototype filter coefficients $F_q(n')$ to obtain the windowed samples $z_q(n')$.

Step 4) Compute the IFFT of size Q of the windowed sample $z_q(n')$ for the n-th sample index of each of the Q subcarriers. This IFFT has to be computed K times, for each sample, to obtain the fragmented samples $y_p(n')$.

Step 5) Recover the core part of the UF-OFDM symbol from the fragmented samples $y_p(n')$.

Step 6) Calculate the prefix part of the UF-OFDM symbol by multiplying the $x_q(n_p)$ samples by the prefix tail coefficients $P_q(n_p)$, and by summing them over each subcarrier index $q \in [\![0, Q-1]\!]$.

Step 7) Calculate the suffix part of the UF-OFDM symbol ($y_{\text{suffix}}(n_s)$) by subtracting the samples of the core part ($y_{\text{core}}(n_s)$) from the samples of the prefix part ($y_{\text{prefix}}(n_s)$) for $n_s \in [\![0, L-2]\!]$.

Step 8) Concatenate the prefix part, the core part and the suffix part to obtain the UF-OFDM symbol.

Note that the generation of the prefix and the core parts being independent, step 4/5 and step 6 can be processed in any order. Only the generation of the suffix part (step 7) requires to first compute the prefix part and the core part of the UF-OFDM symbol.

The proposed UF-OFDM technique generates the UF-OFDM symbol without frequency shift, since it was assumed to be equal to 0 to simplify the development of the equations. When the frequency shift by (k_0 subcarriers) is taken into account, the equation of the frequency shifted UF-OFDM symbol is given by

$$y'(n) = e^{j2\pi \frac{k_0 n}{N}} y(n), n \in [\![0, N+L-2]\!].$$

This additional linear phase rotation would increase the complexity of the transmitter by adding $N+L-1$ complex multipliers. It is however possible to calculate the frequency shifted UF-OFDM symbol more efficiently. Indeed, for the prefix part of the UF-OFDM symbol ($y_{\text{prefix}}(n)$), the linear phase rotation term can be included in the prefix tail coefficients:

$$P_q(n_p) = e^{j2\pi \frac{(q+k_0)n_p}{N}} \sum_{l=0}^{n_p} f_Q(l) e^{-j2\pi \frac{ql}{N}}.$$

Concerning the core part of the UF-OFDM symbol $y_{\text{core}}(n)$, the fragmented samples $y_p(n')$ can be expressed as

$$y_p(n') = e^{j2\pi \frac{k_0 p}{Q}} \sum_{l=0}^{Q-1} (z_q(n') e^{j2\pi \frac{k_0 n'}{N}} e^{j2\pi \frac{qp}{Q}}).$$

The term $\exp[j2\pi(k_0 n')/N]$ can be included in the core filter coefficients $F_q(n)$ and the term $\exp[j2\pi(k_0 p)/Q]$ is equivalent to a circular shift of k_0 samples applied to the inputs of the IFFT of size Q (on the windowed samples $z_q(n)$):

$$y_p(n') = \sum_{q=0}^{Q-1} z_{q-k_0}(n') e^{j2\pi \frac{qp}{Q}},$$

with the filter core coefficients given by

$$F_q(n') = e^{j2\pi \frac{(q+k_0)n'}{N}} \sum_{l=0}^{L-1} (f_Q(l) e^{-j2\pi \frac{ql}{N}}).$$

Therefore, the frequency shift of k_0 subcarriers does not introduce any computational complexity overhead.

B. Adaptation of the proposed technique for any subband size

The technique detailed in Subsection III-A assumes that the total number of subcarriers across all the subbands N can be divided into an integer number of subbands ($\text{mod}_Q(N) = 0$). However, in the particular case of 4G/LTE systems, the minimum allocation size, called a Resource Block (RB), corresponds to 12 subcarriers (frequency) and 7 OFDM symbols (time). Thus, the subband size Q must be equal to a multiple of 12, whereas the IFFT size in 4G/LTE is defined to be a power of 2 in most cases. The only exception concerns the numerology related to the 15 MHz bandwidth case, where the IFFT size is equal to 1536 and the proposed technique can be directly applied for this case since $\text{mod}_{12}(1536) = 0$.

One straightforward solution is to adapt the subband size to satisfy both the simplification constraints and the LTE allocation size. Such condition is satisfied if $Q = 4$, implying that each allocated RB is divided into 3 subbands. However, the spectral confinement and system performance would be negatively affected for such values.

A second solution is to use a subband size that is a power of 2,allocate the information-carrying symbols to the center of the corresponding allocated subbands, and pad with zero-valued samples the edge of the first and last allocated subbands to complete the subband allocation. As an example, if 1 RB must be allocated, then $Q = 16$ and $B = 1$ can be chosen, and $(Q-12)/2 = 2$ zeros must be inserted at the beginning and end of the allocated subbands. More generally, if P corresponds to the minimum allocation size (in number of subcarriers) supported by the communication system ($P = 12$ in 4G/LTE) and N_P is the number of groups of P subcarriers, then, if the subband size Q is fixed, we have

$$B = \left\lceil \frac{N_P \times P}{Q} \right\rceil,$$

$$N_{ZP} = \frac{B \times Q - N_P \times P}{2},$$

where N_{ZP} corresponds to the number of zero valued samples which must be padded at each edge of the allocated subbands. If the number of allocated subbands B is equal to 1, any subband size superior to P can be used and leads to the same spectral confinement as the baseline solution with $Q = P$, since the subband prototype filter coefficients ($f(n)$) do not depend on the subband size Q. However, for a higher number of allocated subbands, the presence of zero-padded samples at the edges of the allocated subbands can impact the spectral confinement and the performance of the system. Thankfully, this solution can be used without performance degradation when $N_{ZP} = 0$, namely when $\text{mod}_Q(N_P \times P) = 0$, but this does not cover all the 4G/LTE RB allocation possibilities.

A third solution is to increase, at the transmitter side, the total number of subcarriers and the frequency sampling by a factor β such that

$$\text{mod}_P(\beta N) = 0, 1 \leq \beta < 2,$$

with $\beta = 1.5$ to support 4G/LTE numerology. The subcarrier spacing being equal to the ratio between the frequency sampling and the total number of subcarriers ($\Delta f = f_s/N$), it remains unchanged (15 kHz for 4G/LTE). The subband size is now a multiple of P, satisfying the condition to employ the proposed technique. Note that this solution does not require changing the frequency sampling and the total number of subcarriers at the receiver side, since it is an oversampling technique. Thus, such solution is transparent for the receiver and is totally compatible with 4G/LTE numerology. Using an IFFT size which is not a power of 2 can be seen as a drawback, but as mentioned in the beginning of this subsection, 4G/LTE numerology requires the support of an IFFT of size 1536 ($= \beta \times 2^{10}$), and the FFT precoder of the Single Carrier (SC) OFDM modulation used in LTE uplink already requires a size that is a multiple of 12 (more precisely, FFT of size $N = 2^a 3^b 5^c \leq 1200$). Furthermore, if $Q \neq 2^n$ can be decomposed into a product such that $Q = Q_N \times R$, with $Q_N = 2^n$ and n, R integers, then it is possible to calculate an IFFT of size Q from R IFFTs of size Q_N as

$$\begin{aligned} x(n) &= \sum_{k=0}^{RQ_N-1} X(k) e^{j2\pi \frac{kn}{RQ_N}} \\ &= \sum_{k=0}^{R-1} e^{j2\pi \frac{kn}{R}} \sum_{l=0}^{Q_N-1} X(kQ_N + l) e^{j2\pi \frac{ln}{Q_N}}. \end{aligned} \quad (20)$$

As an example, if the subband size is set to the 4G/LTE RB size composed of 12 subcarriers, then the IFFT of the subcarrier processing part can be calculated using 3 IFFTs of size 4. The main issue with this solution is that the computational complexity is increased due to the oversampling.

C. Flexibility to support classical OFDM modulation

With the increasing number of scenarios supported in 5G, some applications may require the reuse of the classical OFDM modulation of 4G/LTE in addition to the support of novel multicarrier waveforms such as UF-OFDM. This implies that the transmitter should be able to switch between UF-OFDM and OFDM modulations without major modifications to the computation core, to avoid the duplication of the processing units when considering hardware implementation issues.

In fact, the signal decomposition presented in Subsection III-A can be applied for OFDM. Indeed, the OFDM symbol with the extension of a cyclic prefix of length L can be generated as

$$y(n) = \sum_{k=0}^{N-1} c(k) e^{j2\pi \frac{kn}{N}}, n \in [\![-L, N-1]\!].$$

The signal $y(n)$ can be decomposed into virtual (non-filtered) subbands as

$$\begin{aligned} y(n) &= \sum_{q=0}^{Q-1} \sum_{k=0}^{K-1} c(q + Qk) e^{j2\pi \frac{(q+Qk)n}{N}} \\ &= \sum_{q=0}^{Q-1} e^{j2\pi \frac{qn}{N}} \sum_{k=0}^{K-1} s_k(q) e^{j2\pi \frac{kn}{K}} \\ &= \sum_{q=0}^{Q-1} x_q(n) e^{j2\pi \frac{qn}{K}}. \end{aligned} \quad (21)$$

Similarly to an UF-OFDM symbol, the OFDM symbol can be segmented as

$$y_p(n') = \sum_{q=0}^{Q-1} F'_q(n') x_q(n') e^{j2\pi \frac{qp}{Q}},$$

with

$$F'_q(n') = e^{j2\pi \frac{qn'}{N}},$$

Therefore, the OFDM symbol without the cyclic prefix can be generated by using the equation of the UF-OFDM core part and changing the filter core coefficients to $F'_q(n')$. The cyclic prefix part can be generated by using (17) (step 6 of the method), and is given by

$$y_{\text{prefix}}(n_p) = y(n_p - L) = \sum_{q=0}^{Q-1} x_q(n_p - L) P'_q(n_p), n_p \in [\![0, L-1]\!],$$

with

$$P'_q(n_p) = e^{j2\pi \frac{q(n_p - L))}{N}}.$$

The prefix tail coefficients of the UF-OFDM modulation (16) must be replaced by the $P'_q(n)$ coefficients defined above.

An alternative way to generate the cyclic prefix is simply by copying the last L samples of the core part. This can be done during the recover step (step 5) since it is a concatenation operation. The cyclic prefix can be inserted at the same time, without any complexity increase. Note that, for the two proposed cyclic-prefix insertion methods, the cyclic prefix length in OFDM mode can be different from the filter length

in UF-OFDM mode. The related processing unit just has to be adapted to process the corresponding length.

IV. Computational complexity analysis and comparisons

A. Complexity analysis

We evaluate the computational complexity of the proposed technique in terms of the number of real-valued additions (RAs) and real-valued multiplications (RMs) required to compute one UF-OFDM symbol, and compare it with state-of-the-art approaches for UF-OFDM modulation. We distinguish RAs and RMs because their impact on implementation complexity can differ depending on the type of implementation. For instance, when considering a dedicated hardware implementation, a RM requires more hardware resources (more logic gates) than a RA.

For complex-valued operations, it is necessary to define the number of RMs and RAs required to compute one complex multiplication (CM). We denote by $C_{\text{RM}}(x)$ and $C_{\text{RA}}(x)$ respectively the number of RMs and RAs required for the operation x. Typically, a complex multiplication requires $C_{\text{RM}}(\text{CM}) = 4$ RMs and $C_{\text{RA}}(\text{CM}) = 2$ RAs. But a complex multiplication can be also be counted as $C_{\text{RM}}(\text{CM}) = 3$ RMs and $C_{\text{RA}}(\text{CM}) = 5$ RAs by using the following development:

$$(a+jb)(c+jd) = c(a+b)-b(c+d)+j(c(a+b)+a(d-c)).$$

Furthermore, if a complex sample is multiplied by pre-computed complex coefficients (for instance, filter coefficients), 2 RAs can be removed and $C_{RA}(\text{complexMultiplier}) = 3$. Indeed, if $c + jd$ is the pre-computed complex coefficient, then $c + d$ and $d - c$ can also be pre-computed instead of directly calculated. Since all the complex multiplications of the UF-OFDM techniques involve a pre-computed coefficient, only 3 RAs are required for any complex multiplication. Thus, $C_{\text{RM}}(\text{CM}) = 3$ RMs and $C_{\text{RA}}(\text{CM}) = 3$ are considered in this paper.

In addition, the choice of the IFFT computation technique is another critical aspect when considering complexity, since this choice has a significant impact on the required number of RMs and RAs. A well-known and efficient IFFT computation technique is the split radix IFFT [10], which can be used when the IFFT size is a power of 2 ($N = 2^n$). The computational complexity of the split radix IFFT of size N, refered as $C_{\text{RA/RM}}(\text{IFFT}_N)$, is given by [11]

$$C_{\text{RM}}(\text{IFFT}_N) = N\log_2(N) - 3N + 4,$$

$$C_{\text{RA}}(\text{IFFT}_N) = 3N\log_2(N) - 3N + 4.$$

The computational complexity of the baseline UF-OFDM technique is not considered in this section due to its relatively high complexity when compared to the other presented techniques. This baseline solution is generally presented for understanding and illustrating the UF-OFDM modulation and its specific per-subband filtering. On the other hand, computational complexity analysis of the FD UF-OFDM, the TDW UF-OFDM and the proposed UF-OFDM techniques are derived in the rest of this subsection.

TABLE I
Choice of N_0 depending on the subband size for the FD UF-OFDM technique

Subband size	N_0	NMSE (dB)
12	64	-25.8
16	64	-25.6
48	128	-29.3
64	128	-28

1) FD UF-OFDM complexity analysis: As explained in Subsection II-B, the FD UF-OFDM technique employs multiple small IFFTs of size proportional to N_0 in the oversampled frequency domain (by an oversampling factor N_{OS}) to efficiently process the subband filter. In this section, the oversampling factor N_{OS} is fixed to 2 since this value provides a good trade-off between the signal approximation error and the computational complexity. Thus, the computational complexity of the FD UF-OFDM technique is given by

$$\begin{aligned} C_{\text{RM}}(\text{FD UF-OFDM}) =& B\Big(C_{RM}(\text{FFT}_{N_0}) + C_{\text{RM}}(\text{IFFT}_{2N_0}) \\ &+ 6N_0\Big) + C_{RM}(\text{IFFT}_{2N}), \end{aligned}$$

$$\begin{aligned} C_{\text{RA}}(\text{FD UF-OFDM}) =& B\Big(C_{\text{RA}}(\text{FFT}_{N_0}) + C_{\text{RA}}(\text{IFFT}_{2N_0}) \\ &+ 6N_0\Big) + C_{\text{RA}}(\text{IFFT}_{2N}) \\ &+ 4(B-1)N_0. \end{aligned}$$

Due to the IFFT of size $2N$, the FD UF-OFDM is in any case more computational complex than an OFDM transmitter which only requires an IFFT of size N. Furthermore, the complexity is dependent on the number of allocated subbands and the chosen small IFFT size N_0. For each allocated subband, one FFT of size N_0, one IFFT of size $2N_0$ and $2N_0$ complex multiplications (subband filtering) have to be computed. Thus, the computational complexity increases linearly with the number of allocated subbands. Additionally, when the subband size changes, the choice of N_0 must be reconsidered such that the approximation errors are kept within an acceptable level. The choice of $N_0 = 64$ determined in [8] is applicable for $Q = 12$. However, for other subband sizes, no analysis has been performed in the literature. In order to fairly evaluate the computational complexity, the Normalized Mean Square Error (NMSE) of the approximated UF-OFDM symbol has been evaluated for the subband size of 12, 16, 48 and 64 subcarriers for different N_0 values. Table I shows the N_0 values corresponding to each of these subband sizes for an NMSE inferior to -25 dB, assuming a Dolph-Chebyshev filter [7] with a sidelobe level of 70 dB. This value was chosen to obtain an NMSE level comparable to the one obtained for the case where $Q = 12$ and $N_0 = 64$, to keep an acceptable approximation error. It can be seen from Table I that the N_0 value is only doubled if the subband size is multiplied by 4. This implies that the computational complexity does not increase linearly with the subband

size, contrary to the number of allocated subbands. Thus, it is preferable to use few subbands of large size instead of multiple subbands of short size when considering this technique.

2) TDW UF-OFDM complexity analysis: The complexity of this method mainly depends on the number of windows N_w. A TDW UF-OFDM transmitter using N_w windows will be denoted by TDW_{N_w} UF-OFDM in this section. According to [6], the computational complexity of this technique in terms of number of required RMs and RAs is

$$C_{\text{RM}}(\text{TDW}_{N_w}\ \text{UF-OFDM}) = N_w\Big(C_{RM}(\text{IFFT}_N) + 3(N+L-1)\Big),$$

$$C_{\text{RA}}(\text{TDW}_{N_w}\ \text{UF-OFDM}) = N_w\Big(C_{RA}(\text{IFFT}_N) + 3(N+L-1)\Big) + (N_w-1)(N+L-1).$$

Contrary to the FD UF-OFDM technique, the computational complexity does not increase with the number of allocated subbands B. However, it increases linearly with the number of windows N_w. When only 1 window is used ($N_w = 1$), the computational complexity is close to the one of an IFFT of size N. Thus, the computational complexity is at least N_w times larger than the computational complexity required to compute an OFDM symbol. In the original paper [6], the number of windows N_w considered was set to:

- $N_w = 1$ for the lowest computational complexity, but at the cost of higher approximation errors leading to lower spectral confinement.
- $N_w = 3$ for a good compromise between computational complexity and approximation errors.

In this section, TDW_1 UF-OFDM and TDW_3 UF-OFDM techniques are considered, since $N_w > 3$ leads to a high computational complexity largely undermining the interest of using this technique.

3) Proposed UF-OFDM complexity analysis: Table II shows the number of required RMs and RAs per step (see Subsection III-A for the details of each step) to compute one UF-OFDM symbol using the proposed technique, assuming $\text{mod}_Q(N) = 0$. The total computational complexity in number of RMs and RAs to calculate one UF-OFDM symbol is given by

$$C_{\text{RM/RA}}(\text{UF-OFDM}) = \sum_{i=1}^{8} C_{\text{RM/RA}}(\text{step}_i),$$

$$C_{\text{RM}}(\text{UF-OFDM}) = C_{\text{RM}}(\text{IFFT}_N) + 4(Q+K-1) + 3N\frac{L}{K},$$

$$C_{\text{RA}}(\text{UF-OFDM}) = C_{\text{RA}}(\text{IFFT}_N) + 4(Q+K-1) + 3N\frac{L}{K} + 2L - 1.$$

TABLE II
NUMBER OF REQUIRED RMS AND RAS PER STEP FOR THE PROPOSED UF-OFDM TECHNIQUE.

Step	Operation	C_{RM}	C_{RA}
1	Segmentation	0	0
2	IFFTs of size K	$Q \times C_{\text{RM}}(\text{IFFT}_K)$	$Q \times C_{\text{RA}}(\text{IFFT}_K)$
3	Core windowing	$3Q \times K = 3N$	$3Q \times K = 3N$
4	IFFTs of size Q	$K \times C_{\text{RM}}(\text{IFFT}_Q)$	$K \times C_{\text{RA}}(\text{IFFT}_Q)$
5	Reconstruction	0	0
6	Prefix calculation	$Q \times 3L$	$Q \times 3L$
7	Suffix calculation	0	$2(L-1)$
8	Concatenation	0	0

Similarly to the TDW UF-OFDM technique, the computational complexity does not depend on B, the number of allocated subbands. Furthermore, the computational complexity is equivalent to the one required to compute an OFDM symbol (IFFT of size N) plus an overhead term. This overhead term depends on the ratio between the filter length L and the total number of subbands K ($\alpha = L/K$). In other words, the proposed technique has a computational complexity almost equivalent to OFDM for short subband sizes (for any number of allocated subbands), and the complexity increases with the subband size Q.

When considering any subband size, the oversampling techniques presented in Subsection III-B can be used at the cost of an increase in the computational complexity, as the total number of subcarriers must be multiplied by a factor β ($= 1.5$ for 4G/LTE). Since the IFFT of the subcarrier processing part is no longer a power 2, the split radix FFT technique cannot be directly applied, except if this IFFT is computed using (20) which mostly requires R IFFTs of size Q_N and $(R-1)RQ_N$ complex multiplications by the $\exp[j2\pi(kn)/R]$ terms (for $k \in [\![1, R-1]\!]$). The computational complexity related to the multiplication by the exponential terms can be greatly reduced by noting that $\exp[j2\pi(kn)/R] = 1$ when $\text{mod}_R(n) = 0$, for any $k \in [\![1, R-1]\!]$ values. Thus, $Q/R = Q_N$ complex multiplications can be avoided per k values. In this case, the computation complexity of an IFFT of size $Q = R \times Q_N$ becomes

$$C_{\text{RM}}(\text{IFFT}_{R,Q_N}) = RC_{\text{RM}}(\text{IFFT}_{Q_N}) + 3Q_N(R-1)^2,$$

$$C_{\text{RA}}(\text{IFFT}_{R,Q_N}) = RC_{\text{RA}}(\text{IFFT}_{QN}) + 3Q_N(R-1)^2 + 2(R-1)RQ_N.$$

In this section, only the oversampled solution is considered, as it enables to support any subband size without any restriction, while being less computationally complex than the solution based on multiple intermediate UF-OFDM symbols.

B. Complexity comparison

The computational complexity of the FD UF-OFDM, TDW UF-OFDM and the proposed UF-OFDM are compared with respect to OFDM using the following ratio:

$$\text{Ratio-to-OFDM}_{\text{RM/RA}} = \frac{C_{\text{RM/RA}}(\text{UF-OFDM})}{C_{\text{RM/RA}}(\text{OFDM})},$$

TABLE III
ANALYTICAL EXPRESSION OF THE COMPUTATIONAL COMPLEXITY FOR EACH CONSIDERED UF-OFDM TRANSMITTER

Transmitter	C_{RM}	C_{RA}
OFDM	$N\log_2(N) - 3N + 4$	$3N\log_2(N) - 3N + 4$
FD UF-OFDM	$B\Big(3N_0\log_2(N_0) - N_0 + 8\Big)$ $+ 2N\log_2(2N) - 6N + 4$	$B\Big(9N_0\log_2(N_0) + 7N_0 + 8\Big)$ $+ 6N\log_2(2N) - 6N - 4N_0 + 4$
TDW_{N_w} UF-OFDM	$N_w\Big(N\log_N + 3L + 1\Big)$	$N_w\Big(3N\log_N + N + 4L\Big) - N - L + 1$
Proposed UF-OFDM ($\text{mod}_Q(N) = 0$)	$N\log_2(N) - 3N + 4(Q + K) + 3N\frac{L}{K}$	$3N\log_2(N) - 3N + 4(Q + K) + 3N\frac{L}{K} + 2L - 1$
Proposed UF-OFDM ($\text{mod}_Q(N) \neq 0$)	$\beta N\Big(\log_2(\frac{\beta N}{R}) + 3\Big(\frac{(R-1)^2}{R} + \frac{\beta L}{K} - 1\Big)\Big)$ $+ 4(Q + KR)$	$\beta N\Big(3(\log_2\Big(\frac{\beta N}{R}\Big) + 3\beta\frac{L}{K} + 5R + \frac{3}{R} - 11\Big)$ $+ 4(Q + KR) + 2(\beta L - 1)$

TABLE IV
SELECTED CONFIGURATIONS FOR COMPLEXITY COMPARISON.

	Number of subband allocated B	Subband size Q
Configuration A	1	16
Configuration B	1	64
Configuration C	37	16
Configuration D	9	64
Configuration E	50	12
Configuration F	12	48

where the required numbers of RMs and RAs $C_{\text{RM/RA}}(\text{UF-OFDM})$ are analytically evaluated in the previous subsection for each technique and summarized in Table III. Note that $C_{\text{RM/RA}}(\text{OFDM}) = C_{\text{RM/RA}}(\text{IFFT}_N)$ since an OFDM transmitter only requires an IFFT of size N. Several representative sets of subband sizes and number of allocated subbands must be considered to fairly compare the different UF-OFDM techniques. For this purpose, 6 different configurations are considered. They are detailed in Table IV. For all these configurations, the total number of subcarriers is fixed to 1024 and the length of the subband prototype filter is equal to $L = 73$ samples. Short and large subband sizes are considered to evaluate their impact on the complexity. In addition, subband sizes compatible with a 4G/LTE system are considered for configuration E and F. Configuration A and B represent the cases where only 1 subband is allocated, which is adequate for low data rate services like massive machine communications. Configurations C to F represent the cases where multiple subbands are allocated: the number of allocated subbands is determined such that the entire bandwidth that can be allocated in 4G/LTE is occupied (at most 600 active subcarriers from the total 1024 subcarriers). This corresponds to the extreme cases where a user occupies the totality of the available bandwidth to achieve high date rates.

The computational complexity results are illustrated in Fig. 5a for configuration A. The proposed UF-OFDM technique requires almost the same number of RMs and RAs when compared to the TDW_1 UF-OFDM technique, and only 53% more RMs and 14% more RAs when compared to OFDM. Furthermore, the proposed technique requires 37% less RM and 51% less RAs than the FD UF-OFDM technique. The TDW_3 UF-OFDM technique has the highest computational complexity for this configuration, and is therefore the least interesting technique. When considering configuration B, the proposed UF-OFDM technique requires 13% more RMs when compared to the FD UF-OFDM technique, as shown in Fig. 5b. However, the number of RAs being reduced by 40%, the proposed UF-OFDM technique is still less complex than the FD UF-OFDM technique if the total number of operations is considered (28% less number of RMs and RAs).

Concerning the TDW1 UF-OFDM technique, its complexity reduction comes at the price of an accuracy loss. Thus, the effect of the approximation errors must be considered for a fair comparison. For this purpose, the power spectral densities of the considered UF-OFDM techniques are presented in Fig. 6 for the following parameters:

- allocation of 1 subband of 48 subcarriers,
- use of 1024 subcarriers in total, for a sampling frequency of 15.36 MHz as defined in 4G/LTE,
- application of the Dolph-Chebyshev filter with a sidelobe level of 70 dB.

The OOBPL located outside the allocated subband is higher in the case of the FD UF-OFDM technique by around 5 dB when compared to the proposed technique. As mentioned in [8], this part of the spectrum is not as important as the OOBPL located at each edge of the allocated subband. Indeed, in a practical system, such low OOBPL is never achieved due to the imperfection of the front end components, for instance due to the non-linearity of the power amplifier. Therefore, the approximation errors introduced by the FD UF-OFDM technique do not degrade much the spectral confinement. When considering the TDW UF-OFDM technique, the number of windows has a great impact on the signal approximation and the resulting OOBPL. This is illustrated in Fig. 6, which shows the Power Spectral Density (PSD) of each UF-OFDM transmitter, assuming that the subbands are normalized: the distortion caused by the subband filter is compensated by readjusting the power of each sub-carrier. It can be seen that the use of only 1 window greatly degrades the OOBPL at the edges of the allocated subband. When 3 windows are used, the spectral confinement is improved, but not as much as with the proposed technique: at -40 dB, the frequency difference between the TDW_3 UF-OFDM and the proposed UF-OFDM techniques is around 50 kHz, which is not negligible since it corresponds to more than 3 subcarriers. Thus, a larger guard interval may be required between users to offer the same spectral isolation as the proposed UF-OFDM technique, leading to a data rate loss. A larger number of windows can be employed to reduce the approximation errors, at the cost of

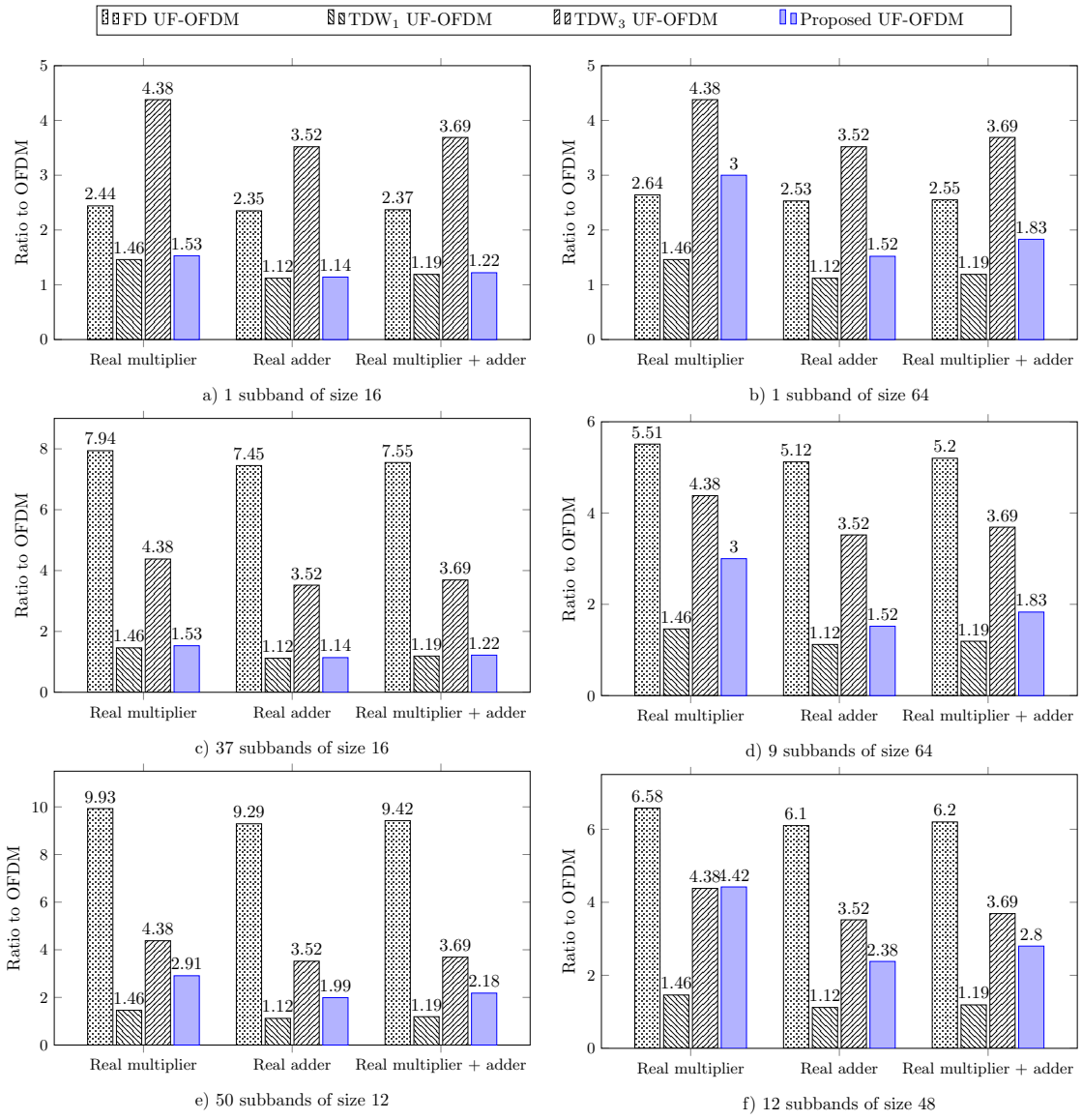

Fig. 5. Computational complexity of the FD UF-OFDM, TDW UF-OFDM and proposed UF-OFDM for different subband configurations.

an increased computational complexity. Concerning the TDW$_1$ UF-OFDM technique, the original signal is highly degraded along with the OOBPL. In fact, the TDW$_1$ UF-OFDM is closer to windowed-OFDM than UF-OFDM.

When considering a subband size of 12 subcarriers for configuration A and a subband of size of 48 subcarriers for configuration B, the same complexity results are obtained. Indeed, Subsection III-B shows that the proposed technique is compatible with any subband size when $B = 1$: the active carriers can be allocated at the middle of the subband, and zero-valued samples can be padded at its extremities. Thus, the proposed UF-OFDM technique is the most interesting technique for $B = 1$, since it has the lowest computational complexity while preserving the signal quality.

Concerning configuration C, the proposed UF-OFDM technique is employed without any oversampling since the total number of subcarriers can be divided into an integer number of

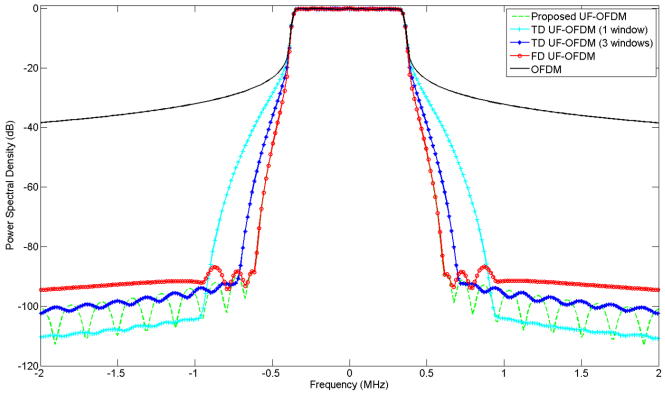

Fig. 6. Power spectral density of the UF-OFDM techniques.

subbands. It can be shown in Fig. 5c shows that the proposed technique has a lower complexity than the FD UF-OFDM and the TDW_3 UF-OFDM techniques. Particularly, the FD UF-OFDM technique requires 4.18 times more RMs and 5.51 times more RA than the proposed UF-OFDM technique. Thus, the FD UF-OFDM loses its appeal when a large number of subbands is employed. When considering a larger subband size with configuration D (Fig. 5d), the proposed UF-OFDM still has a lower complexity than the other techniques, with the exception of the TDW_1 UF-OFDM, which has an unacceptable spectral confinement.

Next, configuration E and F represent cases where multiple subbands are allocated, but the subband size is not a multiple of the total number of subcarriers ($\text{mod}_Q(N) > 0$). In this context, the oversampling technique described in Subsection III-B must be employed for the proposed technique. While this increases the complexity, our proposal still offers reduced complexity when compared to the FD UF-OFDM and to the TDW UF-OFDM techniques, as shown in Fig. 5e and in Fig. 5f.

Therefore, for all the configurations considered, the proposed technique offers significant reductions in computational complexity while preserving the signal accuracy. Note also that the complexity is close to OFDM for a subband size $Q = 16$, regardless of the number of allocated subbands. Finally, our proposed transmitter architecture can be easily adapted to generate an OFDM symbol as demonstrated in Subsection III-C, which is more difficult for techniques like FD UF-OFDM where the IFFT size must be doubled (assuming $N_{OS} = 2$). This is particularly interesting from a hardware implementation perspective, where resources must be shared to reduce the hardware complexity.

Finally, the proposed technique assumes that each subband contains the same number of subcarriers. Therefore, the use of different subband sizes on the same carrier is not directly supported. In fact, for downlink communication, multiple communication services using different numerologies are considered in 5G. For instance, narrow subbands can be employed for mMTC, whereas wider subbands can be used for broadband communication. For the uplink, the user equipment being configured for a particular application, the subband size should be kept constant. Note that the TDW UF-OFDM technique suffers from the same drawback, and only the FD UF-OFDM transmitter can support multiple subband sizes in the same bandwidth. For the latter, the stage of IFFT/FFT (of size N_0) can simply be adapted for a given subband configuration, since subbands are processed separately and independently. In our case, the support of multiple subband sizes can be done by duplicating the transmitter. Assuming that the whole bandwidth is allocated and both subband sizes of 16 and 64 subcarriers must be supported, the proposed transmitter remains 18% to 43% less complex (in number of RM) than the FD UF-OFDM transmitter, despite the replication. These values are obtained by considering the lowest and highest complexity of the FD UF-OFDM transmitter, which correspond to 9 subbands of size 64 and 37 subbands of size 16 respectively. If subbands of size 12 and 48 are considered, the complexity of the proposed transmitter is comparable to the FD UF-OFDM transmitter (between 26% less and 11% more complex).

V. Conclusion

In this paper, a novel UF-OFDM technique with low computational complexity is proposed. One of the main features of this novel technique is that, contrary to the ones proposed in the literature, it does not introduce any approximation of the original signal. Additionally, appropriate solutions have been detailed to support any subband size as defined in 4G/LTE numerology. Comparisons were performed with the techniques presented in the literature using different set of subband allocations and subband sizes. The results show that the proposed UF-OFDM technique provides significant computational complexity reduction in most cases. Finally, power spectral density comparisons were conducted showing that the proposed technique preserves the spectral confinement of UF-OFDM, contrary to the TDW UF-OFDM technique. This demonstrates for the first time the possibility to design a low-complexity UF-OFDM transmitter without any signal degradation, making the UF-OFDM particularly appealing for adoption in upcoming wireless applications and standards.

References

[1] V. Vakilian, T. Wild, F. Schaich, S. ten Brink, and J. F. Frigon, "Universal-filtered multi-carrier technique for wireless systems beyond LTE," in *2013 IEEE Globecom Workshops*, Dec 2013, pp. 223–228.

[2] P. Siohan, Siclet, C., and N. Lacaille, "Analysis and design of OFDM/OQAM systems based on filterbank theory," *IEEE Trans. Signal Process.*, vol. 50, pp. 1170–1183, May 2002.

[3] F. Schaich and T. Wild, "Relaxed synchronization support of universal filtered multi-carrier including autonomous timing advance," in *2014 11th International Symposium on Wireless Communications Systems (ISWCS)*, Aug 2014, pp. 203–208.

[4] T. Hwang *et al.*, "OFDM and Its Wireless Applications: A Survey," *IEEE Transactions on Vehicular Technology*, vol. 58, no. 4, pp. 1673–1694, May 2009.

[5] T. Wild and F. Schaich, "A Reduced Complexity Transmitter for UF-OFDM," in *2015 IEEE 81st Vehicular Technology Conference (VTC Spring)*, May 2015, pp. 1–6.

[6] M. Matthe, D. Zhang, F. Schaich, T. Wild, R. Ahmed, and G. Fettweis, "A Reduced Complexity Time-Domain Transmitter for UF-OFDM," in *2016 IEEE 83rd Vehicular Technology Conference (VTC Spring)*, May 2016, pp. 1–5.

[7] T. W. Parks and C. S. Burrus, *Digital Filter Design*. New York: John Wiley & Sons, 1987, ch. 7.

[8] M. Mukherjee, L. Shu, V. Kumar, P. Kumar, and R. Matam, "Reduced out-of-band radiation-based filter optimization for UFMC systems in 5G," in *2015 International Wireless Communications and Mobile Computing Conference (IWCMC)*, Aug 2015, pp. 1150–1155.

[9] X. Wang, T. Wild, and F. Schaich, "Filter Optimization for Carrier-Frequency and Timing-Offset in Universal Filtered Multi-Carrier Systems," in *2015 IEEE 81st Vehicular Technology Conference (VTC Spring)*, May 2015, pp. 1–6.

[10] P. Duhamel and H. Hollmann, "Split radix FFT algorithm," *Electronics Letters*, vol. 20, pp. 14–16, January 1984.

[11] H. Sorensen, M. Heideman, and C. Burrus, "On computing the split-radix FFT," *IEEE Transactions on Acoustics, Speech, and Signal Processing*, vol. 34, no. 1, pp. 152–156, Feb 1986.